Published in
Physica status solidi (c) 6, supplement 2, S818-821, 2009
which should be used for any reference to this work

Monolithically integrated UV/IR-photodetectors based on an AlN/GaN-based superlattice grown on an AlGaN buffer layer

Daniel Hofstetter[*, 1], Esther Baumann[1], Fabrizio R. Giorgetta[1], Ricardo Théron[1], Fabien Guillot[2], Eva Monroy[2], Sebastian Golka[3], and Gottfried Strasser[3]

[1] Institute of Physics, University of Neuchâtel, 2000 Neuchâtel, Switzerland
[2] CEA-Grenoble, INAC/SP2M/NPSC, 17 rue des Martyrs, 38054 Grenoble, France
[3] Centre of Micro- and Nanostructures, Technical University of Vienna, Floragasse 7, 1040 Vienna, Austria

In this article, we demonstrate closely spaced, monolithically integrated photodetectors in two largely different wavelength ranges. The epitaxial structure of the devices was grown by plasma-assisted molecular-beam epitaxy on an AlN-on-sapphire template; it consists of a Si-doped AlGaN thin film, and a nearly strain compensated 40 period AlN/GaN superlattice with 1.0 nm thick GaN quantum wells and 2.0 nm thick AlN barriers. The entire structure is covered with an AlGaN cap layer. The superlattice acts as active region for the infrared detector, while the AlGaN buffer layer serves as active area for the ultraviolet detector. While the photovoltaic near-infrared detector has a center wavelength of 1.37 µm, the photoconductive ultraviolet detector has a long wavelength cutoff at 250 nm. The two detectors could be operated up to room temperature with reasonable sensitivities.

1 Introduction Multi-spectral cameras operating in wavelength ranges as different as the ultraviolet (UV), the visible, or even the infrared (IR) are attracting substantial interest for applications in surveillance, failure analysis, and meteorology [1]. One particularly interesting application is the detection of defective insulators in high power electric transmission lines, where even a microscopic crack in the ceramic material can eventually result in considerable system damage. However, it is known that such cracks cause a corona being visible only in the UV; at the same time, the insulator will heat up excessively, leading to IR radiation. Therefore, an elegant method to catch such problems as early as possible is the use of cameras being sensitive in different spectral ranges. Up to this point, the fabrication concept of multi-spectral imaging systems for this type of failure analysis was based on overlaying visible and UV pictures coming from two different image sensor arrays. Although this solution offers obviously optimized performances for both wavelength ranges, it requires the use of several bulky and rather expensive optical components. Therefore, the entire system suffers from very high prices on the market. In addition, such a system is relatively sensitive for shocks or vibrations, and therefore not 100% reliable for in-the-field applications. For all these reasons, a monolithic integration of two or even three operation wavelengths into a single camera chip could offer great advantages over existing solutions, notably in terms of price, robustness, and flexibility. It is clear, however, that there are not many semiconductor materials which would allow a monolithic integration of detectors in all three wavelength ranges required here. In addition, most semiconductors having sufficiently dissimilar bandgap energies show rather large lattice mismatches on the order of several percent, even within the same family [2]. Nevertheless, several approaches – mostly using interband and intraband transitions – have been fabricated. Successful dem-

[*] Corresponding author: e-mail Daniel.Hofstetter@unine.ch

onstrations include solutions based on AlGaN/GaN [3], Si/p-Si [4], and GaAs/p-GaAs layer stacks [5] using interband absorption for the shorter detection wavelength and free-carrier absorption for the longer wavelength. In addition, multi-color detectors based on bias voltage switching and using excited states in either quantum dots or minibands have been proposed and characterized [6-8]. Here, we present a slightly different solution involving both optical interband and intersubband transitions. Compared to the earlier approaches, this method is appealing because of its straight-forward tailorability and the possibility to measure the required signals simultaneously in different wavelength ranges. This will have a positive effect on the acquisition speed of large multi-spectral images. Our solution is based on the monolithic integration of a photoconductive UV interband detector based on an AlGaN thin film [9] and a photovoltaic near-IR intersubband detector based on an AlN/GaN superlattice [10-12]. As a first demonstrator, we present here a UV/IR detector pair with only 350 µm spatial separation between the UV and IR device. The two detectors exhibit spectrally narrow responsivity curves, thus enlarging the UV-to-visible rejection ratio in the case of the UV device, and improving the noise behavior in case of the IR detector.

2 Fabrication The layer structure of this dual-band photodetector was grown by plasma-assisted molecular beam epitaxy on a commercial AlN-on-sapphire template. It consisted of a 250 nm-thick Si-doped ([Si] ~ 5 x 10^{19} cm^{-3}) $Al_{0.65}Ga_{0.35}N$ thin film, followed by a regular 40 period superlattice with 1.0 nm-thick Si-doped GaN quantum wells ([Si] ~ 1 x 10^{19} cm^{-3}) and 2.0 nm-thick AlN barriers. Finally, the epitaxial layer structure was covered with a 5 nm-thick $Al_{0.65}Ga_{0.35}N$ cap layer. Obviously, the doping of the buffer layer is not really necessary (neither for the UV detector, nor for the IR detector); in future experiments, we therefore plan to work with a nominally undoped buffer. In a practical device, however, some residual doping will always be present: the level of this doping is usually sufficiently high to produce a useful ohmic contact, but sufficiently low to reduce the dark current in the UV detector to a minimum. The wafer was then mesa-structured to a depth of roughly 150 nm using reactive ion etching. UV detectors were subsequently defined in areas where the superlattice had been removed down to the $Al_{0.65}Ga_{0.35}N$ buffer layer. In this most simple configuration, they consist of two simple, rectangularly shaped, alloyed ohmic metal contacts (Ti/Al/Ti/Au, 20/170/5/500 nm) with a dimension of 50 x 100 μm^2. As reference contact, one could very well use an ohmic contact to the AlGaN buffer layer; the only role of this contact is indeed to provide a voltage reference point. On the other hand, the IR detectors are fabricated from rectangularly shaped Schottky contacts of 50 x 100 μm^2 size (Ti/Au, 10/500 nm) evaporated directly on the as-grown areas.

Electrical connections between the detector contact pads and the larger ceramic contacts on the chip holder were obtained by wire bonding. A schematic cross-section through the layer structure showing the relative positions of the devices is shown in Fig. 1, while in Fig. 2, a typical microscope picture of the chip with the corresponding bonding wires is presented. As shown by the scaling bar, the separation between the UV and the IR devices is 350 µm.

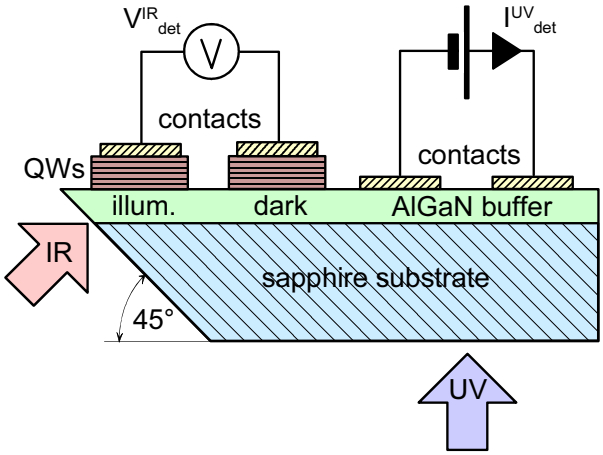

Figure 1 Schematic cross section through the sample showing the relative positions of the UV and the IR detector. The QWs are used as detection layer for the IR, while the AlGaN buffer is the detection layer for the UV radiation.

As usual in IR-detectors based on intersubband transitions, vertical incidence is allowed as long as an optical diffraction grating on the detector surface re-directs the light into the direction of the epitaxial layers. In the present state, we have preferred a simpler coupling scheme via a 45 ° wedge. The comb structures also shown in Fig. 2 have nothing to do with the present experiments and were not further characterized.

3 Characterization

3.1 UV detector The UV sensitive part of this dual-band photo-detector functions like a photoconductor. A bias voltage is applied between its two contacts; and in an ideal situation with no doping in the active layer, no current would flow between them. As already mentioned, in most practical cases, some residual doping will be present; and therefore, a small dark current will flow. Under excitation with UV light, additional electrons and holes will be generated leading to a substantial photo-current flow between the biased contacts of the device. A common problem in such AlGaN photo-detectors is their slow response. It can be explained by a long hole trapping time which causes a minority recombination time being considerably longer than the electron transit time. The positive side of this effect is a photo-conductive gain, but the negative one is the slow response [12]. For the characterization of the UV detector, a Fourier transform spectrometer equipped with an external deuterium lamp, and a CaF_2 beam splitter was utilized. In order to adapt to the slow response of the UV detector, the beam of the UV lamp was chopped at low

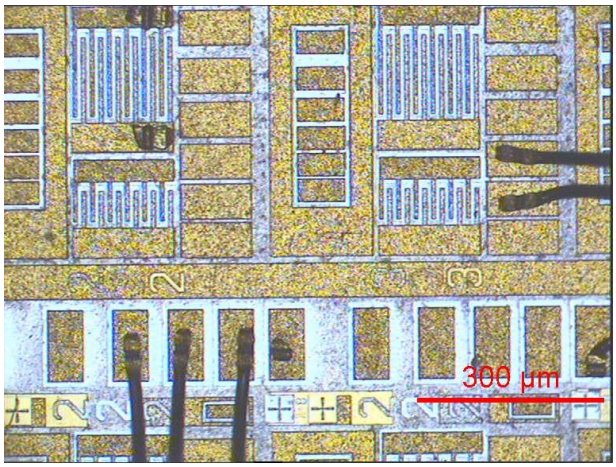

Figure 2 Microscope photograph of the sample showing the bonded detectors and their separation on the chip. The device with three bond wires at the bottom is the IR detector, while the one with only two wires at the right is the UV detector. The comb contacts were not used in these experiments.

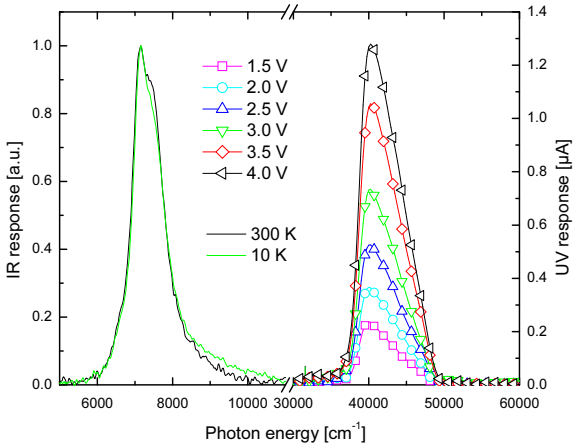

Figure 3 Measured spectral responsivity curves for the UV (1.5 to 4.0 V in steps of 0.5 V at 300 K) and the IR detector (10 and 300 K).

frequency (f = 6.66 Hz), and focalized onto the detector from the substrate side. The electrical signal produced was then amplified in a lock-in amplifier and fed into the external detector port of the spectrometer. The necessary bias voltage to operate the UV detector in a photoconductive mode was provided by a Keithley sourcemeter. Again due to the slow response time of the UV detector, the measurements were performed in step-scan modulation using a dwell time on the order of 500 ms. Measurements at 6 different bias voltages ranging from 1.5 V to 4 V were recorded at room temperature.

3.2 IR detector For reasons of convenience, two equally sized mesa contacts were used to form the IR-detector. There is, however, absolutely no necessity to do so. For instance, the dark reference could have been chosen as a contact sitting on the AlGaN buffer and being far away from the illuminated contact.

Characterization of the IR detector was based on illumination of only one of the two contacts of the device via a 45 ° polished facet using an internal white light source, and the CaF_2 beam splitter of the Fourier spectrometer. In a more application-driven experiment, the dark contact would sit far enough from the illuminated contacts so that the asymmetry in illumination could still be maintained. As described in our earlier publication [13], the asymmetric shape of the QWs in the nitride material system is the real driving force for seeing a photovoltaic response from these detectors. Under optical excitation, microscopic displacements of many dopant electrons result in dipoles which will add up to an appreciable photovoltage. Acquisition of the photovoltaic signal was accomplished via an SR570 amplifier, and direct feeding of the amplified voltage into the external port of the spectrometer. Spectra were taken at various temperatures between 10 K and room temperature with the sample being mounted in a liquid He flow cryostat. Figure 3 shows the optical characteristics of the two detectors. The spectra of the IR device recorded at temperatures of 10, 50, 100, 150, 200, 250, and 300 K show about 10 % difference in responsivity; therefore, only the 10 K and the 300 K spectrum are presented. The responsivity peak position is at 7280 cm^{-1} (910 meV, 1.37 µm) with a full width at half maximum of 925 cm^{-1} (116 meV).

Based on our earlier experience with photoconductors, we tested the UV device at room temperature only. As expected, it shows a pronounced signal increase with increasing bias voltage. The responsivity peaks at a value of 40000 cm^{-1} which corresponds to 5 eV or 250 nm. Its full width at half maximum is roughly 5000 cm^{-1} (0.67 meV). We observe a long wavelength cut-off at about 4.9 eV which is mainly determined by the bandgap of the AlGaN active layer. On the other hand, the short wavelength cut-off at 6.2 eV is due to strong band-to-band absorption in the underlying AlN growth template layer. A much sharper cut-off on the short wavelength side and thus a considerably narrower responsivity peak could most likely be achieved by introduction of an additional AlGaN layer with a higher Al content. When illuminating the device from the back, such an additional AlGaN filter layer would also prevent most undesired UV radiation from reaching the IR detector. In addition, the surface grating to be fabricated on top of the IR device would be an efficient reflector only for long wavelengths, and therefore serve as an additional wavelength filter preventing us from seeing a parasitic signal on the IR detector. The voltage responsivity of the IR detector was determined to lie in the 10 V/W range, while the best current responsivity of the UV device amounts to roughly 10 mA/W. In future measurements and based on experiments with more recently grown epitaxial material, we expect substantial improvements of these values.

In conclusion, a monolithic integration of a solar-blind UV detector and a narrowband near-IR detector was dem-

onstrated. With these devices being functional up to room temperature and being separated by only 350 μm, we believe to having given a first hint on what AlGaN multilayer structures could be capable in the future. In any case, this demonstration is an important step towards multispectral cameras containing in each pixel UV, near-visible, and IR sensitive imaging elements.

Acknowledgements The authors would like to thank the European project NitWave (#004170), and the Professorship Program and the NCCR "Quantum Photonics" both sponsored by the Swiss National Science Foundation. AlN-on-sapphire templates were provided by DOWA Electronics Materials Inc.

References

[1] See for instance http://www.ofil.co.il/Products/range_of_products.html
[2] S. T. Strite and H. Morkoc, J. Vac. Sci. Technol. B **10**, 1237 (1992).
[3] G. Ariyawansa, M. B. M. Rinzan, M. Alevli, M. Strassburg, N. Dietz, A. G. U. Perera, S. G. Matsik, A. Asghar, I. T. Ferguson, H. Luo, A. Bezinger, and H. C. Liu, Appl. Phys. Lett. **89**, 091113 (2006).
[4] G. Ariyawansa, M. B. M. Rinzan, S. G. Matsik, G. Hastings, A. G. U. Perera, H. C. Liu, M. Buchanan, G. I. Sproule, V. I. Gavrilenko, and V. P. Kuznetsov, Appl. Phys. Lett. **89**, 061112 (2006).
[5] G. Ariyawansa, M. B. M. Rinzan, D. G. Esaev, S. G. Matsik, G. Hastings, A. G. U. Perera, H. C. Liu, B. N. Zvonkov, and V. I. Gavrilenko, Appl. Phys. Lett. **86**, 143510 (2005).
[6] J. Li, K. K. Choi, and D. C. Tsui, Appl. Phys. Lett. **86**, 211114 (2005).
[7] G. Ariyawansa, V. Apalkov, A. G. U. Perera, S. G. Matsik, G. Huang, and P. Bhattacharya, Appl. Phys. Lett. **92**, 111104 (2008).
[8] A. Majumdar, K. K. Choi, J. L. Reno, and D. C. Tsui, Appl. Phys. Lett. **86**, 261110 (2005).
[9] E. Monroy, F. Calle, E. Munoz, E. Omnes, B. Beaumont, and P. Gibart, J. Electron. Mater. **28**, 240 (1998).
[10] D. Hofstetter, S.-S. Schad, H. Wu, W. J. Schaff, and L. F. Eastman, Appl. Phys. Lett. **83**, 572 (2003).
[11] D. Hofstetter, E. Baumann, F. R. Giorgetta, M. Graf, M. Maier, F. Guillot, E. Bellet-Amalric, and E. Monroy, Appl. Phys. Lett. **88**, 121112 (2006).
[12] J. Singh, Semiconductor Optoeletronics: Physics and Technology (McGraw-Hill, New York, 1995).
[13] D. Hofstetter, E. Baumann, F. R. Giorgetta, F. Guillot, S. Leconte, and E. Monroy, Appl. Phys. Lett. **91**, 131115 (2007).